

TAS3 miR390-dependent loci in non-vascular land plants: towards a comprehensive reconstruction of the gene evolutionary history

Sergey Y. Morozov¹, Irina A. Milyutina¹, Tatiana N. Erokhina², Liudmila V. Ozerova³, Alexey V. Troitsky¹ and Andrey G. Solovyev^{1,4}

¹ Belozerky Institute of Physico-Chemical Biology, Moscow State University, Moscow, Russia

² Shemyakin-Ovchinnikov Institute of Bioorganic Chemistry, Russian Academy of Science, Moscow, Russia

³ Tsitsin Main Botanical Garden, Russian Academy of Science, Moscow, Russia

⁴ Institute of Molecular Medicine, Sechenov First Moscow State Medical University, Moscow, Russia

ABSTRACT

Trans-acting small interfering RNAs (ta-siRNAs) are transcribed from protein non-coding genomic TAS loci and belong to a plant-specific class of endogenous small RNAs. These siRNAs have been found to regulate gene expression in most taxa including seed plants, gymnosperms, ferns and mosses. In this study, bioinformatic and experimental PCR-based approaches were used as tools to analyze TAS3 and TAS6 loci in transcriptomes and genomic DNAs from representatives of evolutionary distant non-vascular plant taxa such as Bryophyta, Marchantiophyta and Anthocerotophyta. We revealed previously undiscovered TAS3 loci in plant classes Sphagnopsida and Anthocerotopsida, as well as TAS6 loci in Bryophyta classes Tetraphidiopsida, Polytrichopsida, Andreaeopsida and Takakiopsida. These data further unveil the evolutionary pathway of the miR390-dependent TAS3 loci in land plants. We also identified charophyte alga sequences coding for SUPPRESSOR OF GENE SILENCING 3 (SGS3), which is required for generation of ta-siRNAs in plants, and hypothesized that the appearance of TAS3-related sequences could take place at a very early step in evolutionary transition from charophyte algae to an earliest common ancestor of land plants.

Submitted 19 February 2018
Accepted 28 March 2018
Published 16 April 2018

Corresponding author

Sergey Y. Morozov,
morozov@genebee.msu.su

Academic editor
Yegor Vassetzky

Additional Information and
Declarations can be found on
page 19

DOI 10.7717/peerj.4636

© Copyright
2018 Morozov et al.

Distributed under
Creative Commons CC-BY 4.0

OPEN ACCESS

Subjects Bioinformatics, Genomics, Molecular Biology, Plant Science

Keywords Silencing, Trans-acting RNA, Small interfering RNA, ARF genes, Micro RNA, Charophyte algae, Bryophytes

INTRODUCTION

Plant chromosomal loci of trans-acting small interfering RNAs (ta-siRNAs) and microRNAs (miRNAs) encode non-protein-coding and protein-coding precursor transcripts, which are synthesized by RNA polymerase II and include cap-structures and poly-(A) tails. In plants, primary miRNA transcripts forming internal imperfect hairpins are processed by a protein complex including Dicer-like protein 1 (DCL1), HYL1 and SERRATE to give RNA duplexes with 2-nucleotide 3'-overhangs, which are then terminally methylated by specific RNA methylase HEN1. One strand of such duplexes, being typically of 21 nucleotides in

length and representing a mature miRNA, is selectively recruited by Argonaut (AGO) family protein to an effector complex targeting a specific RNA for AGO-mediated endonucleolytic cleavage or translational repression ([Rogers & Chen, 2013](#); [Axtell, 2013](#); [Bologna & Voinnet, 2014](#); [Borges & Martienssen, 2015](#); [Chorostecki et al., 2017](#)).

Some specific microRNAs are able to initiate production of ta-siRNAs (and other secondary phased RNAs—phasiRNAs) by an step-by-step processing of long double-stranded RNA by DCL4 from a start point defined by miRNA-directed cleavage of a single-stranded RNA precursor in a “phased” pattern. These PHAS loci include non-coding TAS genes and genes encoding penta-tripeptide repeat-containing proteins (PPRs), nucleotide-binding and leucine-rich repeat-containing proteins (NB-LRRs), or MYB transcription factors ([Allen & Howell, 2010](#); [Zhai et al., 2011](#); [Xia et al., 2013](#); [Fei, Xia & Meyers, 2013](#); [Axtell, 2013](#); [Yoshikawa, 2013](#); [Zheng et al., 2015](#); [Komiya, 2017](#); [Liu et al., 2018](#); [Deng et al., 2018](#)). Biogenesis of ta-siRNAs includes initial AGO-dependent miRNA binding at single or dual sites of the precursor transcripts and their subsequent cleavage. The further process is dependent on plant RNA-dependent RNA polymerase 6 (RDR6) and SGS3 proteins participating in the formation of dsRNA, which is then cleaved in a sequential and phased manner by DCL4 with assistance of DRB4 (dsRNA binding protein). The resulting ta-siRNAs (mostly of 21 bp in length), similar to miRNAs, are methylated by HEN1 protein ([Allen & Howell, 2010](#); [Axtell, 2013](#); [Fei, Xia & Meyers, 2013](#); [Yoshikawa, 2013](#); [Bologna & Voinnet, 2014](#); [Komiya, 2017](#); [Deng et al., 2018](#)).

Arabidopsis TAS3a transcript, first identified by [Allen et al. \(2005\)](#), gives rise to two near-identical 21-nucleotide tasiARFs targeting the mRNAs of some auxin-responsive transcription factors (ARF2, ARF3/ETT and ARF4). Most angiosperm TAS3 primary transcripts are recognized by miR390 and cleaved by AGO7 at the 3' target site, whereas the 5' miRNA target site is non-cleavable. However, the number of miR390 cleavage sites, organization of tasiARF sequence blocks and phasing registers may vary among different TAS3 genes of vascular plants ([Allen & Howell, 2010](#); [Axtell, 2013](#); [Fei, Xia & Meyers, 2013](#); [Zheng et al., 2015](#); [Xia et al., 2013](#); [Xia, Xu & Meyers, 2017](#); [De Felippe et al., 2017](#); [Komiya, 2017](#); [Deng et al., 2018](#)). Moreover, miR390 may additionally target and inhibit protein-coding gene transcripts, such as StCDPK1 related to auxin-responsive pathway ([Santin et al., 2017](#)).

Previously, we described a new method for identification of plant TAS3 loci based on PCR with a pair of oligodeoxyribonucleotide primers mimicking miR390. The method was found to be efficient for dicotyledonous plants, cycads, conifers, and mosses ([Krasnikova et al., 2009](#); [Krasnikova et al., 2011](#); [Krasnikova et al., 2013](#); [Ozerova et al., 2013](#)). Importantly, at that time the structural and functional information on bryophyte TAS3 loci was available only for the model plant *Physcomitrella patens* ([Arif, Frank & Khraiwesh, 2013](#)), and we used our PCR-based approach as a phylogenetic profiling tool to identify relatives of *P. patens* TAS3 loci in 26 additional moss species of class Bryopsida and several mosses of classes Polytrichopsida, Tetraphidopsida and Andreaeopsida. Moreover, we found a putative pre-miR390 genomic sequence for an additional moss class, Oedipodipsida ([Krasnikova et al., 2013](#)). Our studies revealed that a representative of Marchantiophyta (liverwort *Marchantia polymorpha*, class Marchantiopsida) could also encode a candidate miR390 gene

and a potential TAS3-like locus ([Krasnikova et al., 2013](#)). This finding extended the known evolutionary history of TAS3 loci to the proposed most basal land plant lineage ([Ruhfel et al., 2014](#); [Bowman et al., 2017](#)). In addition, we sequenced putative pre-miR390 genomic locus for *Harpanthus flotovianus* (Marchantiophyta, class Jungermanniopsida) ([Krasnikova et al., 2013](#)). Later, our findings of TAS3-like and miR390 loci were experimentally confirmed in the studies of the transcriptomes of Marchantiophyta plants *M. polymorpha* ([Lin et al., 2016](#); [Tsuzuki et al., 2016](#)) and *Pellia endiviifolia* (class Jungermanniopsida) ([Alaba et al., 2015](#)).

New genomic and transcriptomic sequence data for basal Viridiplantae appeared in NCBI (<http://ncbi.nlm.nih.gov/sra>) and Phytozome (<http://www.phytozome.net>) databases prompted us to perform new experimental and *in silico* analyses of TAS3 loci in basal taxons of Viridiplantae. In this paper, we identified previously unrecognized TAS3 loci in classes Sphagnopsida and Anthocerotopsida, as well as composite TAS6/TAS3 loci in classes Tetraphidiopsida, Polytrichopsida, Andreaeopsida and Takakiopsida. Additionally, we revealed SGS3-coding sequences in charophytes and analyzed their evolutionary links.

MATERIALS AND METHODS

Dried material for *Sphagnum angustifolium* and *S. girgensohnii* were taken from herbarium at Department of Biology, Moscow State University. Total DNA was extracted from dry plants using the Nucleospin Plant Extraction Kit (Macherey-Nagel, Düren, Germany) according to the protocol of the manufacturer. For PCR amplification, the following degenerate primers were used: a forward primer Spha-TASP (5'-GGCGRTAWCCYACTGAGCTA-3') and reverse primer Spha-TASM (5'-TAGCTCAGGAGRGATAMMBMRA-3'). For PCR, 30 cycles were used with a melting temperature of 94 °C –3', and the next steps are as follows: an annealing temperature 94 °C –20", 65 °C –20", 58 °C –30", and an extending temperature of 72 °C followed by a final extension at 72 °C for 5'. PCR products were separated by electrophoresis of samples in a 1.5% agarose gel and purified using the Gel Extraction Kit (Qiagen, Hilden, Germany). For cloning, the PCR-amplified DNA bands isolated from gel were ligated into pGEM-T (Promega, Madison, WI, USA). The resulting clones were screened by length in 1,5% agarose gel. The plasmids were used as templates in sequencing reactions with an automated sequencer (Applied Biosystems, Foster City, CA, USA) 3730 DNA Analyzer with facilities of “Genom” (Moscow, Russia).

Sequences for comparative analysis were retrieved from NCBI (<http://www.ncbi.nlm.nih.gov/>), Phytozome (<http://www.phytozome.net>) and 1,000 Plant Transcriptome Project (“1KP”) (<http://1kp-project.com/blast.html>). Sequence similarities were analysed by NCBI Blast at <http://blast.ncbi.nlm.nih.gov/BlastAlign.cgi>. The presence of open reading frames within retrieved sequences was analysed at <http://web.expasy.org/translate/>. The nucleic acid sequences and deduced amino acid sequences were analyzed and assembled using the NCBI. Conserved domains in the amino acid sequences SGS3 were identified using the CD-Search of the NCBI.

The sequences of SGS3 protein and TAS3 nucleotide sequences were aligned by MAFFT version 7 software ([Katoh & Standley, 2014](#)). The phylogenetic tree was constructed by the

Neighbor-Joining method with 1,000 bootstrap replications in MEGA7 ([Kumar, Stecher & Tamura, 2016](#)). The evolutionary distances were computed using the JTT matrix-based method and are in the units of the number of amino acid substitutions per site. The rate variation among sites was modeled with a gamma distribution (shape parameter = 1).

RESULTS

TAS3 loci in Bryophyta (classes Sphagnopsida and Takakiopsida)

It is commonly accepted that mosses of classes Sphagnopsida and Takakiopsida represent most basal lineages in Bryophyta ([Shaw et al., 2010](#); [Shaw, Szövényi & Shaw, 2011](#); [Rosato et al., 2016](#)). Previously, using primers, which have allowed us to detect pre-miR390 and TAS3 loci in Bryopsida and some other moss classes, we failed to identify pre-miR390 and TAS3 genes in genus *Sphagnum* ([Krasnikova et al., 2013](#)). However, a predicted sequence of pri-miR390 from *Sphagnum fallax* was recently reported ([Xia, Xu & Meyers, 2017](#)). This finding prompted us to re-evaluate the occurrence of TAS3-like loci in Sphagnopsida. To this end, we designed a new pair of degenerated PCR primers Spha-TASP and Spha-TASM, which differed from those used previously ([Krasnikova et al., 2011](#); [Krasnikova et al., 2013](#)). As a positive control, we used plasmid DNA carrying cloned TAS3 gene of *Andreaea rupestris*, a representative of basal Bryophyta ([Krasnikova et al., 2013](#)). Like the positive control, two total DNA probes from *Sphagnum angustifolium* and *S. girgensohnii* gave a single main PCR product of the expected size ([Fig. 1](#)). Cloning and sequencing of these PCR fragments revealed two TAS3-like primary structures having 285 (*S. angustifolium*) and 292 (*S. girgensohnii*) bases in length and exhibiting 96% identity (*e*-value = 2e–131). We named these loci as Sphan-285 and Sphgi-292, ([Fig. 2](#), [Fig. S1](#) and [Table 1](#)). Despite that the degenerate miR390-mimicking primers were used for amplification of these loci, miR390 recognition sites in TAS3 species well corresponded to genomic loci of TAS3 extracted from genomic and transcriptomic data of other plants from genus *Sphagnum* ([Fig. 2](#)).

Peatmosses *S. angustifolium* and *S. girgensohnii* belong to subgenera *Cuspidata* and *Acutifolia*, respectively ([Shaw et al., 2010](#); [Shaw et al., 2016](#)). To extend search for TAS3-like loci inside genus *Sphagnum* we performed bioinformatics analysis of the nucleotide sequences in databases available at NCBI (Sequence Read Archive) and Phytozome (version 12.1). Phytozome has recently released genome assembly of bog moss *S. fallax* (version 0.5). Bog moss belongs to subgenus *Cuspidata* and represents the most closely related moss to *S. angustifolium* ([Shaw et al., 2016](#)). BLASTN search at Phytozome allowed us to reveal a TAS3-like locus (supercontig super_37), which has 100% identity to the TAS3 locus of *S. angustifolium* sequenced in this study ([Fig. S1](#) and [Table 1](#)). Unexpectedly, we found an additional TAS3-like locus in *S. fallax* (transcript Sphfalx0293s0011, supercontig super_293). This TAS3 locus in bog moss has 277 nucleotides in length and showed only a distant relation to the *S. angustifolium* TAS3 ([Fig. 2](#), [Fig. S1](#) and [Table 1](#)).

To further analyze Sphagnopsida TAS3-related loci, we used BLAST analysis of Sequence Read Archive (SRA), which is the NCBI database collecting sequence data obtained by the use of next generation sequence (NGS) technology. Assembly of sequence reads of *S. recurvum* (subgenus *Cuspidata*) retrieved by BLAST search using *S. fallax* sequences as

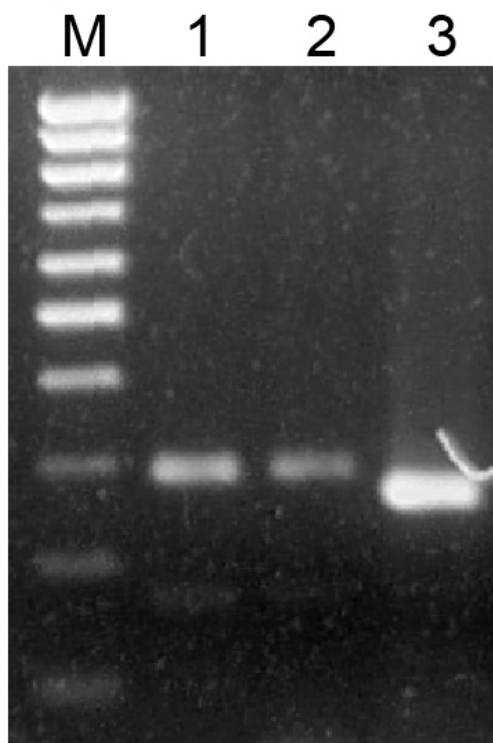


Figure 1 Analysis of PCR products in 1.5% agarose gel. Amplification of genomic DNA sequences flanked by miR390 and miR390* sites. PCR products were obtained on genomic DNAs with degenerate primers. *Sphagnum angustifolium* (1), *Sphagnum girgensohnii* (2), *Andreaea rupestris* (3). (M), DNA size markers including bands ranging from 100 bp to 1,000 bp with 100 bp step (Sibenzyme).

Full-size DOI: 10.7717/peerj.4636/fig-1

queries revealed two TAS3 loci (Table 1). The first locus (Sphre-283) is 283 nucleotides in length and has 98% identity to Sphan-285. The second locus (Sphre-277) shows 98% identity to Sphfalx0293s0011 (Table 1, Fig. S1). These findings indicate that two distant TAS3 loci in species of a particular subgenus of genus *Sphagnum* are extremely similar.

We also analyzed the SRA database of subgenus *Sphagnum* (Shaw et al., 2010; Shaw et al., 2016). It was found that *S. magellanicum* belonging to this subgenus also encode two TAS3 loci called Sphma-285 (285 nt size) and Sphma-286 (286 nt size) (Fig. S1 and Table 1). Unlike *S. fallax* and *S. recurvum*, in *S. magellanicum* TAS3 loci are more similar, showing 86% identity (Fig. 2). Both Sphma-285 and Sphma-286 had 85% identity to Sphan-285 (Fig. 2). It was found that TAS3-like locus (Sphpa) from one more representative of subgenus *Sphagnum* (*S. palustre*) exhibited 98% identity to Sphma-285 (Fig. S1 and Table 1). The SRA database also contained sequence reads of two representatives from subgenus *Subsecunda* (Shaw et al., 2010; Shaw et al., 2016). Our BLAST analysis and subsequent assembly of retrieved reads revealed a single TAS3 locus in *S. cribrosum* (Sphcri, 291 nt size) showing 95% identity to Sphan-285 and 81% identity to Sphma-286 (Fig. 2, Fig. S1 and Table 1) and a partial TAS3-like sequence in *S. lescurii* (Fig. S1 and Table 1).

Analysis of the SRA database of *Takakia lepidozoides* (class Takakiopsida) allowed us to reveal only one TAS3-like sequence (Takle-207) (Fig. S1 and Table 1). The same sequence

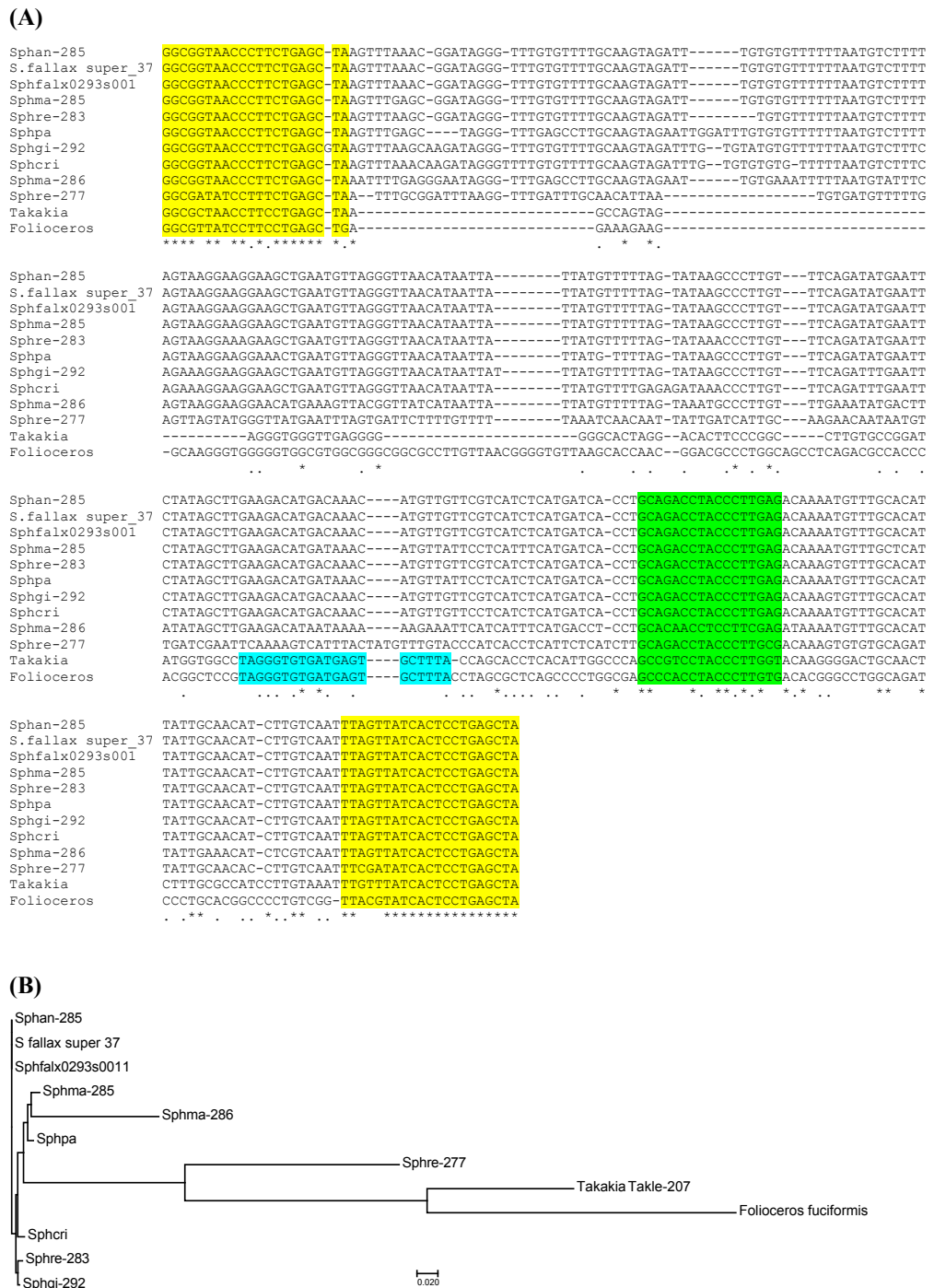


Figure 2 Analysis of TAS3 loci in genus *Sphagnum*. (A) Multiple sequence alignment of available nucleotide sequences of TAS3-like loci from mosses of genus *Sphagnum* along with TAS3 loci of *Takakia lepidozoides* and *Folioceros fuciformis*. Alignment was generated at MAFFT6 program. The miR390 target sites are in yellow, and putative tasiARF-a2 site is in green; tasiAP2 site is in blue. (B) The minimal evolution phylogenetic tree based on analysis of the aligned TAS3 genes from mosses of genus *Sphagnum*. This tree was generated according MAFFT6 program. For full plant names and accession numbers see Table 1.

Full-size DOI: 10.7717/peerj.4636/fig-2

Table 1 List of the putative TAS3 loci in Sphagnopsida and Takakiopsida.

Plant species	Locus name	Subgenus	Length	Sequence source
<i>Sphagnum angustifolium</i>	Sphan-285	<i>Cuspidata</i>	285 nts	MF682529
<i>S. girgensohnii</i>	Sphgi-292	<i>Acutifolia</i>	292 nts	MF682530
<i>S. fallax</i>	contig super_37	<i>Cuspidata</i>	285 nts	SRX2120232
<i>S. fallax</i>	Sphfalx0293s0011	<i>Cuspidata</i>	277 nts	Sphfalx0293s0011 ^a
<i>S. recurvum</i>	Sphre-283	<i>Cuspidata</i>	283 nts	SRX1513231
<i>S. recurvum</i>	Sphre-277	<i>Cuspidata</i>	277 nts	SRX1513231
<i>S. magellanicum</i>	Sphma-285	<i>Sphagnum</i>	285 nts	SRX2330962
<i>S. magellanicum</i>	Sphma-286	<i>Sphagnum</i>	286 nts	SRX2330962
<i>S. palustre</i>	Sphpa	<i>Sphagnum</i>	partial	SRX1516347
<i>S. cibrosum</i>	Sphcri	<i>Subsecunda</i>	291 nts	ERX443237
<i>S. lescurii</i>	Sphle	<i>Subsecunda</i>	partial	ERX337183
<i>Takakia lepidozioides</i>	Takle-207	Not applicable	207 nts	ERX2100030 SKQD-2076588 ^b

Notes.^aPHYTOZOME accession.^b1 KP accession ([Xia, Xu & Meyers, 2017](#)).

was revealed in a longer assembly which was found recently upon search of 1KP database ([Xia, Xu & Meyers, 2017](#)).

Since Takakiopsida and Sphagnopsida are most basal sister lines to all other Bryophyta ([Shaw et al., 2010](#); [Shaw, Szövényi & Shaw, 2011](#); [Rosato et al., 2016](#); [Puttick et al., 2018](#)), it was very interesting to compare the structural organization of Takakiopsida and Sphagnopsida TAS3 loci with other classes of Bryophyta. Our previous detailed analysis of approximately 40 TAS3 loci in Bryophyta ([Krasnikova et al., 2011](#); [Krasnikova et al., 2013](#)) showed that the general structure of moss TAS3 is similar in all taxa and fits the structural organization of *Physcomitrella patens* genes, comprising dual miR390 target sites on the 5' and 3' borders and internal monomeric tasiAP2 sequence followed by tasiARF sequence positioned in 20–30 bases. We revealed that phylogenetic tree of TAS3-like loci in Bryophyta showed clear subdivision of their sequences into two main clades (see Fig 5 in [Krasnikova et al., 2013](#)). The first group was formed by a cluster of sequences close to *P. patens* TAS3 species PpTAS3a, PpTAS3d, and PpTAS3f, and the second one—by those close to PpTAS3b, PpTAS3c, and PpTAS3e. The recent paper on the structure of TAS3 loci in lower land plants ([Xia, Xu & Meyers, 2017](#)) has shown the structure-functional basis for this phylogenetic subdivision. TAS3 species of the first group (PpTAS3a/PpTAS3d/PpTAS3f cluster) were shown to form class III of TAS3-like loci and contain, in addition to the previously reported tasiAP2 and tasiARF-a2 sequences, newly discovered tasiARF-a3 sequence positioned 5' according to tasiAP2 (Fig. 3). Among TAS3 species of basal Bryophyta, *Andreaea rupestris* locus 13-Aru ([Krasnikova et al., 2013](#)) belongs to class III (Fig. 3).

BLAST comparison of *T. lepidozioides* TAS3 with known Bryopsida loci showed that Takle-207 belongs to class II of TAS3 with typical positioning of tasiAP2 and tasiARF-a2 sequences (Fig. 2 and Fig. S1). On the other hand, none of Sphagnopsida TAS3-like sequences (Table 1) showed conventional internal structural organization

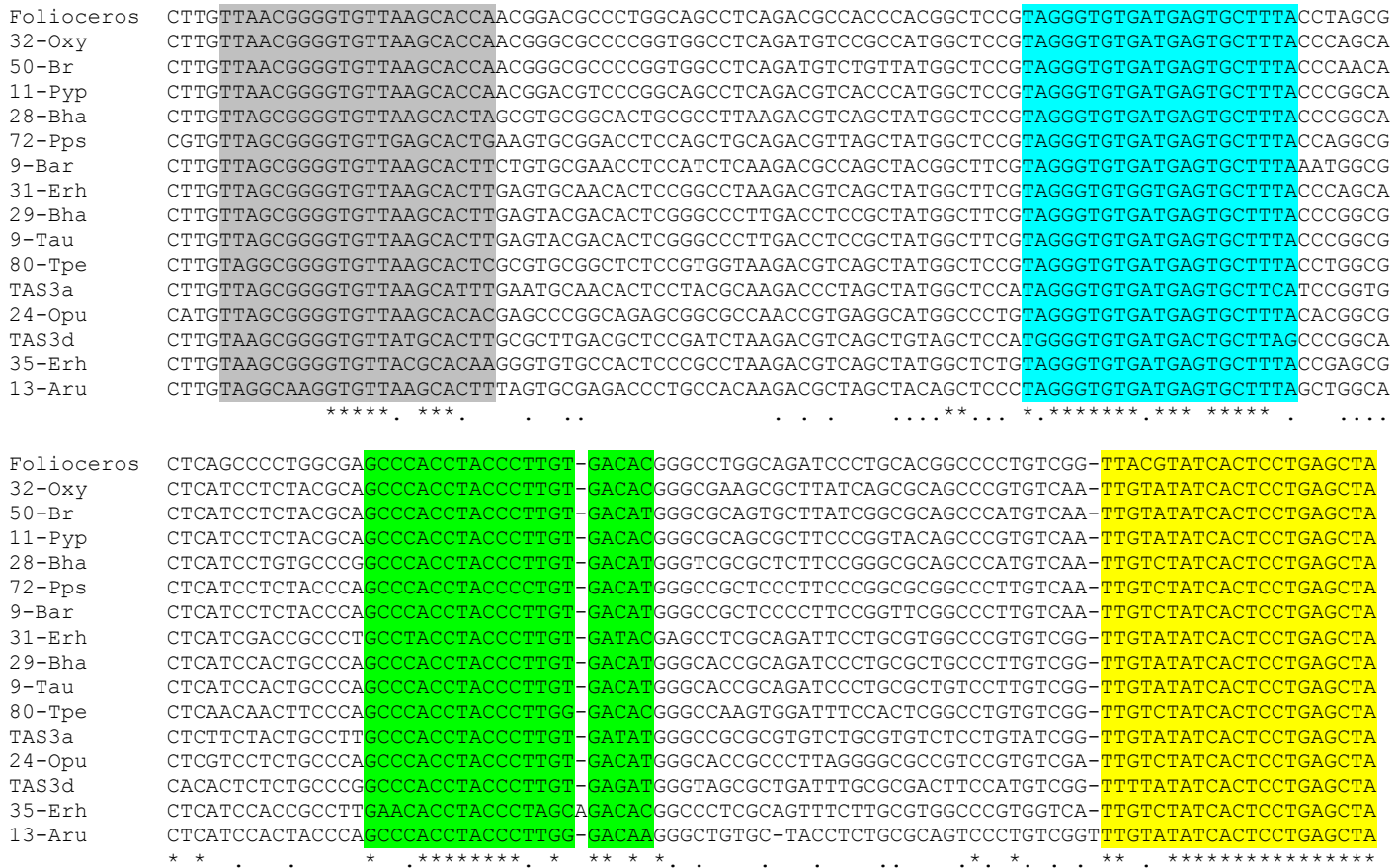


Figure 3 Multiple sequence alignment of selected available nucleotide sequences of class III TAS3-like loci from Bryopsida mosses along with TAS3 locus of *Folioceros fuciformis*. Alignment was generated at MAFFT6 program. The miR390 target sites are in yellow; putative tasiARF-a2 site is in green; tasiAP2 is in blue, and tasiARF-a3 is shaded. Note that all sequences are cut in the 5'-terminal TAS3 area to exclude non-aligned regions.

Full-size DOI: 10.7717/peerj.4636/fig-3

of the most moss TAS3 species. The only recognizable conserved site, except miR390-targeting regions, was identified as tasiARF-a2 sequence, which was found to be conserved between two very distant TAS3 loci in *S. fallax* and *S. recurvum* (Fig. 2). The mentioned above tasiARF sequences, tasiARF-a2 and tasiARF-a3, showed no sequence similarity suggesting their independent origins. These tasiRNAs were found to be formed from different strands of the TAS3 dsRNA intermediate and target different regions of ARF genes (Xia, Xu & Meyers, 2017). Inhibition of production of both tasiARF RNAs in *P. patens* resulted in obvious developmental defects exhibited, in particular, as alterations in gametophore initiation, protonemal branch determinacy and caulonemal differentiation (Plavskin et al., 2016).

Comparison of nucleotide sequences between TAS3 species of several moss classes revealed in many plants obvious similarity of nucleotide sequence blocks including tasiAP2 site and immediate upstream 21 bp block occurring in the same 21-bp-phase (Fig. 4A). We hypothesized that this sequence block may correspond to novel previously unrecognized

(A)

<i>Andreaea1</i>	AAGACGTCA _G C _T TATGGCTCCG	TAGGGTGTGATGAGTGCTTTA	43
<i>Andreaea2</i>	AAGACGT _T A _G C _T CCG	TAGGGTGTGATGAGTGCTTTA	190
<i>Tetraphis1</i>	AAGACGTCA _G C _T TATGGCTCCG	TAGGGTGTGATGAGTGCTTTA	137
<i>Tetraphis2</i>	AAGACGTCA _G C _T TATGGCTCCG	TAGGGTGTGATGAGTGCTTTA	182
<i>Tetraphis3</i>	AAGACGCCAGCTATGGCTCCG	TAGGGTGTGATGAGTGCTTTA	440
<i>Plagiomnium</i>	AAGACGTCA _G C _T TATGGCTCCG	TAGGGTGTGATGAGTGCTTTA	315
<i>Leucobryum</i>	AAGACGTCA _G C _T TATGGCTCCG	TAGGGTGTGATGAGTGCTTTA	1006
<i>Racomitrium</i>	AAGACGTCA _G C _T TATGGCTCCG	TAGGGTGTGATGAGTGCTTTA	304
<i>Philonotis</i>	AAGACGTCA _G C _T TATGGCTCCG	TAGGGTGTGATGAGTGCTTTA	314
<i>Dicranum</i>	AAGACGTCA _G C _T TATGGCTCCG	TAGGGTGTGATGAGTGCTTTA	58
<i>Encalypta</i>	AAGACGTCA _G C _T TATGGCTCCG	TAGGGTGTGATGAGTGCTTTA	1009
<i>Ceratodon</i>	AAGACGTCA _G C _T TATGGCTCCG	TAGGGTGTGATGAGTGCTTTA	192
<i>Niphotrichum</i>	AAGACGTCA _G C _T TATGGCTCCG	TAGGGTGTGATGAGTGCTTTA	455
<i>Funaria</i>	AAGACGTCA _G C _T TATGGCTCCG	TAGGGTGTGATGAGTGCTTTA	250
<i>Schwetschkeop</i>	AAGACGTCA _G C _T TATGGCTCCG	TAGGGTGTGATGAGTGCTTTA	1632
<i>Aulacomnium</i>	AAGACGTCA _G C _T TATGGCTCCG	TAGGGTGTGATGAGTGCTTTA	278
<i>Syntrichia</i>	AAGACGTCA _G C _T TATGGCTCCG	TAGGGTGTGATGAGTGCTTTA	154
<i>Diphystrum1</i>	AAGACGTCA _G C _T TATGGCTCCG	TAGGGTGTGATGAGTGCTTTA	047
<i>Diphystrum2</i>	AAGACGTCA _G C _T TATGGCTCCG	TAGGGTGTGATGAGTGCTTTA	486
<i>Pohlia</i>	AAGACGCCAGCTATGGCTCCG	TAGGGTGTGATGAGTGCTTTA	38
<i>Bryum</i>	AAGACGCCAGCTACGGCTTC	TAGGGTGTGATGAGTGCTTTA	240
<i>PHYSCO TAS3A</i>	AAGACCTA _G C _T TATGGCTCCG	TAGGGTGTGATGAGTGCTTTA	158

(B)

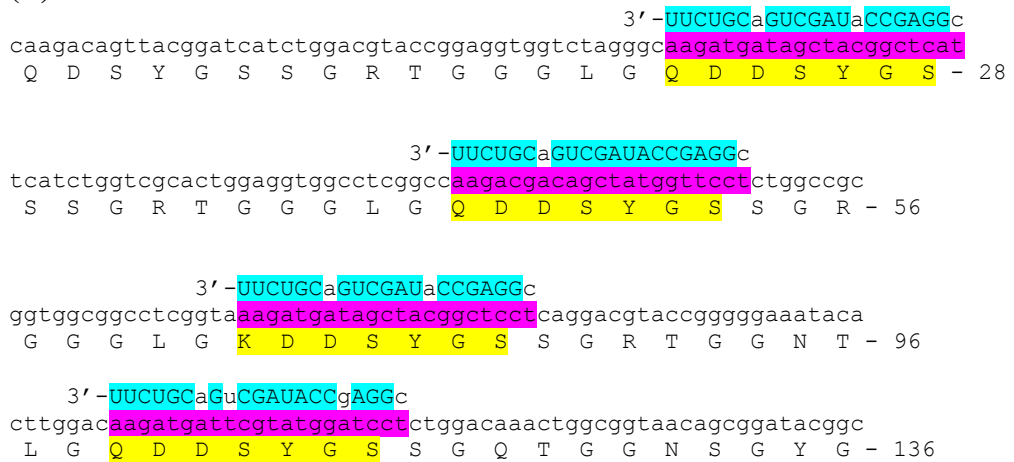


Figure 4 Novel potential ta-siRNA in Bryopsida plants. (A) Multiple sequence alignments of nucleotide sequence blocks including tasiAP2 site and preceding 21 bp site of putative ta-siRNA of *Andreaea rupestris* TAS3-like locus WOGB_2010369 with the corresponding transcript sequences of moss TAS3 loci. BLASTN was used at 1 KP blast site. For the complete TAS3 transcript sequences see [Xia, Xu & Meyers, 2017](#). The putative tasiAP2 site is in blue, and preceding putative ta-siRNA site is in violet. *Andreaea1* - *Andreaea rupestris* WOGB_2010369; *Andreaea2* - *Andreaea rupestris* WOGB_2002765; *Tetraphis1* - *Tetraphis pellucida* HVBQ_2019753; *Tetraphis2* - *Tetraphis pellucida* HVBQ_2011866; *Tetraphis3* - *Tetraphis pellucida* HVBQ_2005644; *Plagiomnium* - *Plagiomnium insigne* BGXB_2010105; *Leucobryum* - *Leucobryum glaucum* RGKL_2062694; *Racomitrium* - *Racomitrium varium* RDOO_2117129; *Philonotis* - *Philonotis fontana* ORKS_2058791; *Dicranum* - *Dicranum scoparium* NGTD_2078536; *Encalypta* - *Encalypta streptocarpa* KEFD_2058811; (continued on next page...)

Full-size DOI: 10.7717/peerj.4636/fig-4

Figure 4 (...continued)

Ceratodon - *Ceratodon_purpureus* FFPD_2044193; Niphotrichum - *Niphotrichum_elongatum* ABCD_2000143; Funaria - *Funaria* sp. XWHK_2042016; Schwetschkeop - *Schwetschkeopsis fabronia* IGUH_2166854; Aulacomnium - *Aulacomnium_heterostichum* WNGH_2088134; Syntrichia - *Syntrichia_princeps* GRKU_2074985; Diphyscium1 - *Diphyscium_foliosum* AWOI_2069791; Diphyscium2 - *Diphyscium_foliosum* AWOI_2006305; Pohlia - *Pohlia_nutans* GACA01023180; Bryum argenteum - Unigene33538 GCZP01053768; PHYSCO TAS3A - *Physcomitrella patens* TAS3a BK005825. (B) The example target transcript sequence (lower case letters) from *Leucobryum albidum* (VMXJ_2127900) is presented alongside with the predicted novel ta-siRNA shown in blue and above the transcript. Lower case letters in ta-siRNA indicate non-Watson-Crick pairing positions. Complementary mRNA sequences are in violet; conserved amino acid sequence signatures are in yellow. Numbers indicate codon positions of the target gene.

ta-siRNA in many moss species. This putative siRNA in its single-stranded form really presents in *P. patens* transcriptome as minus-sense 21-nucleotide ta-siRNA (see NCBI SRA accessions [SRX903096–SRX903105](#)) like tasiARF RNA ([Arif et al., 2012](#)). Thus, we speculated that novel hypothetical ta-siRNA might be produced from TAS3, and its minus-strand is complementary to uncharacterized well-conserved, protein-coding moss mRNAs which have homologs also in conifers and angiosperms ([Fig. 4B](#); [Fig. S2](#)).

TAS3 loci in Anthocerotophyta

Taking into account the finding of TAS3-like loci in classes Sphagnopsida and Takakiopsida and previously published data ([Krasnikova et al., 2013](#); [Xia, Xu & Meyers, 2017](#)), one can conclude that the only remaining blind-spot in land plants with respect to TAS3 is represented by phylum Anthocerotophyta. Relationships between liverworts, mosses and hornworts are still obscure. Moreover, the question remains which bryophyte phylum is a sister line to all other land plants ([Qiu, 2008](#); [Shaw, Szövényi & Shaw, 2011](#); [Harrison, 2017](#); [Puttick et al., 2018](#)). Recent molecular phylogenetic analysis, in which three bryophyte lineages were resolved, revealed that a clade with mosses and liverworts could form a sister group to the tracheophytes, whereas the hornworts is sister line to all other land plants ([Wickett et al., 2014](#)). However, analyses of the plastid genome sequences suggested another branching order of the phylogenetic tree, with hornworts rather than moss/liverwort clade being a sister group to tracheophytes ([Lewis, Mishler & Vilgalys, 1997](#); [Samigullin et al., 2002](#); [Ruhfel et al., 2014](#); [Lemieux, Otis & Turmel, 2016](#)). Moreover, some very recent nuclear gene comparisons also suggested that hornworts could be a sister clade to tracheophytes, and liverworts plus mosses might be closer to a common ancestor of land plants ([Rosato et al., 2016](#); [Bowman et al., 2017](#)). However, this ancestor could have more tracheophyte-like characteristics than Setaphytida (liverworts/mosses) due to secondary simplification in liverworts ([Puttick et al., 2018](#)).

Analysis of the SRA database of Anthocerotophyta revealed a putative TAS3-like sequence in *Folioceros fuciformis* (family Anthocerotaceae). Unexpectedly, the discovered TAS3-like sequence (Folfu) was found to be 244 nucleotides in length and obviously similar to Bryophyta class III TAS3 species ([Fig. 3](#), [Fig. S3](#) and [Table 2](#)). The identity of Folfu to some moss TAS3 sequences exceeds 80% being therefore even higher than between some related Bryopsida species ([Fig. 3](#)). Thus these data clearly indicate a close relation of TAS3 in Anthocerotophyta to Bryophyta TAS3 (excepting Sphagnopsida).

Table 2 List of the putative TAS3 loci in Anthocerotophyta and Marchantiophyta.

Plant species	Class/subclass	Order	Length	Sequence source
<i>Folioceros fuciformis</i>	Anthocerotopsida/Anthocerotidae	Anthocerotales	244 nts	SRS2162722
<i>Marchantia polymorpha</i> 1-Mpo	Marchantiopsida/Marchantiidae	Marchantiales	256 nts	KC812742
<i>Marchantia emarginata</i>	Marchantiopsida/Marchantiidae	Marchantiales	262 nts	SRX1952816
<i>Conocephalum japonicum</i>	Marchantiopsida/Marchantiidae	Marchantiales	252 nts	SRX1952810
<i>Ricciocarpus natans</i>	Marchantiopsida/Marchantiidae	Marchantiales	235 nts	ERX337127
<i>Dumontiera hirsuta</i>	Marchantiopsida/Marchantiidae	Marchantiales	243 nts	SRX1126014
<i>Plagiochasma appendiculatum</i>	Marchantiopsida/Marchantiidae	Marchantiales	247 nts	SRX1741567
<i>Conocephalum conicum</i>	Marchantiopsida/Marchantiidae	Marchantiales	248 nts	ILBQ_2006554 ^a
<i>Lunularia cruciata</i>	Marchantiopsida/Marchantiidae	Lunulariales	220 nts	TXVB_2071521 ^a
<i>Marchantia paleaceae</i>	Marchantiopsida/Marchantiidae	Marchantiales	257 nts	HMHL_2051051 ^a
<i>Metzgeria crassipilis</i>	Jungermanniopsida/Metzgeriidae	Metzgeriales	226 nts	ERX337128
<i>Pellia endiviifolia</i>	Jungermanniopsida/Pelliidae	Pelliiales	192 nts	SRX726500

Notes.

^a1 KP accession ([Xia, Xu & Meyers, 2017](#)).

TAS3 loci in Marchantiophyta

Some of the recent molecular phylogenetic reconstructions suggested that Marchantiophyta species could represent a sister clade to all other land plants (see above). Therefore, finding and comparative analyses of TAS3 loci in this taxon represented a significant interest for understanding early events in TAS3 evolution. In contrast to class Marchantiopsida, where putative TAS3 and pre-miR390 loci were previously identified ([Krasnikova et al., 2013](#); [Lin et al., 2016](#); [Tsuzuki et al., 2016](#)), for class Jungermanniopsida only potential pre-miR390 loci were found in *Pellia endiviifolia* and *Harpanthus flotovianus* ([Krasnikova et al., 2013](#); [Alaba et al., 2015](#)). Assuming that miR390 was found to be among eight most conserved miRNA species in land plants ([Xia et al., 2013](#); [You et al., 2017](#); [Liu et al., 2018](#)), Jungermanniopsida could be expected to encode TAS3 loci.

To detect new potential TAS3 loci, we performed BLAST analysis of the SRA database for species of class Jungermanniopsida using *Marchantia polymorpha* TAS3 sequence (1-Mpo) as a query. Using this approach we revealed a set of reads and assembled a single TAS3-like locus (Pelen-192) for *Pellia endiviifolia* (192 nt size). In addition, TAS3 locus of 226 nucleotides in length was found in *Metzgeria crassipilis* (Metcr-226) ([Fig. 5, Table 2](#), [Fig. S3](#)). The latter locus was also recently revealed in a search of 1KP database ([Xia, Xu & Meyers, 2017](#)).

TAS3 1-Mpo sequence was further used for BLAST analysis of other Marchantiopsida sequences available at the NCBI SRA database. As a result, we retrieved sequence reads and assembled five full-length TAS3-like sequences in *Plagiochasma appendiculatum* (Plaap-247), *Dumontiera hirsuta* (Dumhi-243), *Marchantia emarginata* (Marem-262), *Ricciocarpus natans* (Ricna-235) and *Conocephalum japonicum* (Conja-252) ([Fig. 5, Table 2](#), [Fig. S3](#)). Recent bioinformatics analysis of 1KP database revealed three additional full-length TAS3-like sequences in *Conocephalum conicum*, *Lunularia cruciata* and *Marchantia paleaceae*.

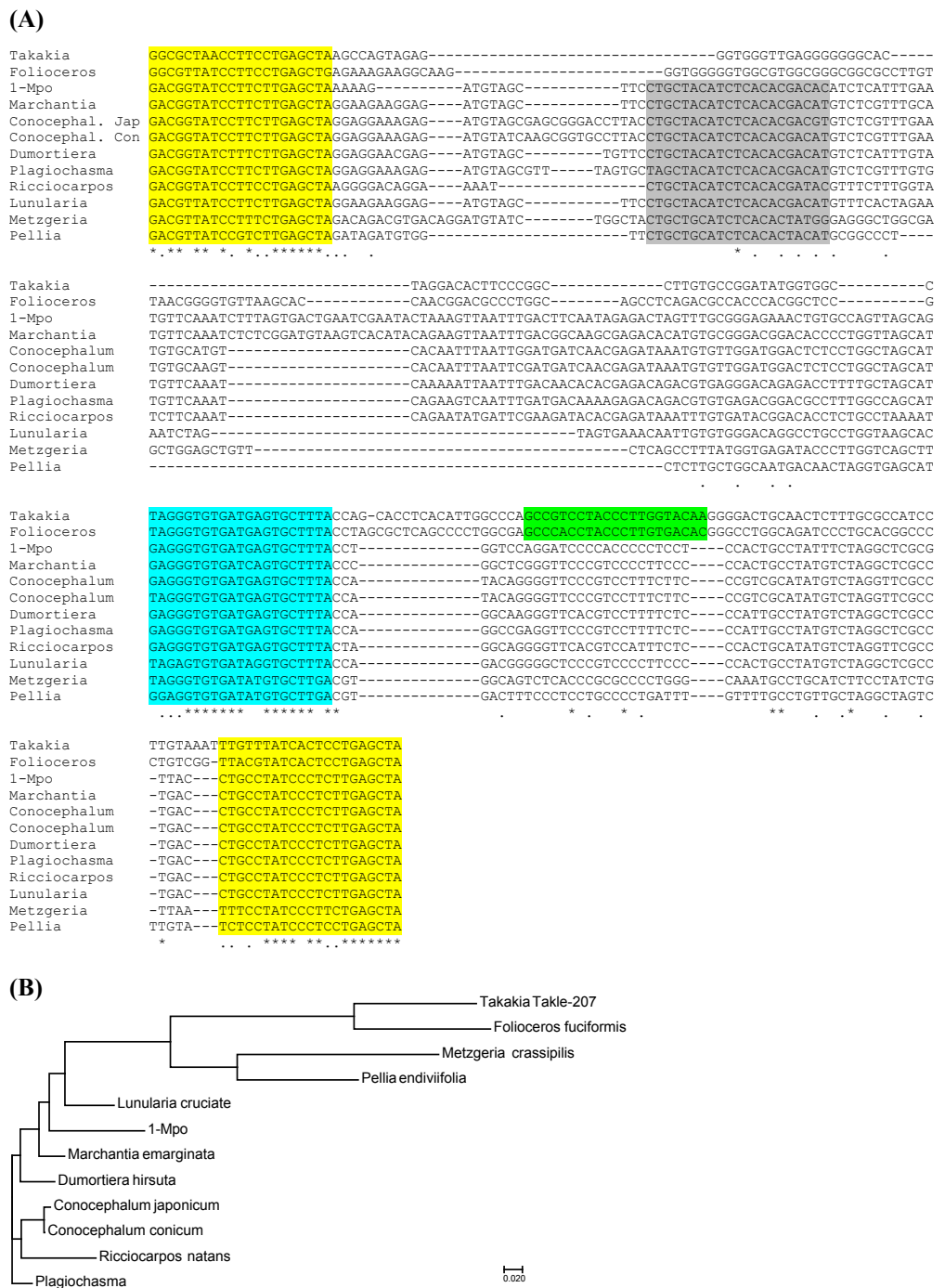


Figure 5 Analysis of TAS3 loci in Marchantiophyta plants. (A) Multiple sequence alignment of available nucleotide sequences of TAS3-like loci from Marchantiophyta plants along with TAS3 loci of *Takakia lepidozoides* and *Folioceros fuciformis*. Alignment was generated at MAFFT6 program. The miR390 target sites are in yellow, and putative tasiARF-a2 site is in green; tasiAP2 site is in blue. (B) The minimal evolution phylogenetic tree based on analysis of the aligned TAS3 genes from Marchantiophyta plants. This tree was generated according MAFFT6 program. For full plant names and accession numbers see Table 2.

Full-size DOI: 10.7717/peerj.4636/fig-5

([Xia, Xu & Meyers, 2017](#)) ([Table 2](#)). Thus, totally 11 TAS3-like loci have been found in Marchantiophyta.

TAS6 loci in Bryophyta

Previous studies of *P. patens* revealed three novel non-coding PHAS loci (TAS6) which were located in rather close genomic proximity to PpTAS3 loci (PpTAS3a, PpTAS3d, and PpTAS3f) and expressed as common RNA precursors with these TAS3 species ([Cho, Coruh & Axtell, 2012](#); [Arif et al., 2012](#); [Arif, Frank & Khraiwesh, 2013](#)). Moreover, miR529 and miR156 were suggested to influence accumulation of ta-siRNAs specific not only for TAS6, but also for PpTAS3a ([Cho, Coruh & Axtell, 2012](#)). We have found that localization of TAS6 loci close to TAS3 genes in common transcripts was not unique for *P. patens* (subclass Funariidae), since these loci were also found to be encoded by three other mosses of subclasses Bryidae and Dicranidae ([Krasnikova et al., 2013](#)).

For further search of the combined TAS6/TAS3 loci, we performed bioinformatics analysis of 1KP database. Although nucleotide sequences of miR156 and related miR529, as well as their recognition sites in RNA transcripts, are highly conserved among land plants ([Morea et al., 2016](#); [Axtell & Meyers, 2018](#)), the internal sequences between dual miR156/miR529 recognition sites show little or no similarity even between different TAS6 loci of *P. patens* ([Arif et al., 2012](#)). So we used, as queries for BLAST search, the individual full-length TAS6/TAS3 loci including most characterized locus encoding PpTAS3a ([Fig. 6](#)), as well as those for PpTAS3d and PpTAS3f. First, it was found that in addition to four previously found Bryopsida species, encoding TAS6/TAS3 loci, these loci could be revealed in basal subclasses Timmiidae (*Timmia austriaca*) and Diphysciidae (*Diphyscium foliosum*) ([Shaw, Szövényi & Shaw, 2011](#); [Table 3, Fig. S4](#)). List of TAS6/TAS3 loci in other moss subclasses was also significantly extended: we found 18 new loci in Bryidae, seven loci in Dicranidae and four loci in Funariidae ([Table 3, Fig. S4](#)). These novel loci showed recognizable but varying sequence similarities to the PpTAS3a-containing locus ([Fig. 6](#)). Second, most importantly, putative TAS6/TAS3 loci were revealed in four basal classes of Bryophyta, namely, Tetraphidopsida, Polytrichopsida, Andreaeopsida and Takakiopsida ([Table 3, Fig. S4](#)). These novel loci had a similar organization to Bryopsida TAS6/TAS3 species ([Fig. 6](#)). However, no TAS6-specific sequence signatures were found in the vicinity of genomic *S. fallax* and *M. polymorpha* TAS3 loci upon analysis of the corresponding Phytozome genome contigs.

Phylogeny of SGS3 as a characteristic molecular component of TAS3 pathway

It was shown that some species of green algae could encode ancient types of dicer-like proteins, RDRs, and AGOs. On the other hand, no encoded SGS3 proteins were revealed for these algae ([Zheng et al., 2015](#)). Since SGS3 was found to be essential for production of tasiARF RNAs in moss *P. patens* ([Plavskin et al., 2016](#)), we performed sequence analyses to identify possible SGS3 genes in charophytes. For identification of SGS3 protein orthologs among land nonvascular plants and charophytes, we used as a query the most conserved region of *P. patens* SGS3 including short zinc binding zf-XS domain and RNA recognition

2058811 *Encalypta streptocarpa* (accession KEFD_ 2058811)

2058791 *Philonotis fontana* (accession ORKS_2058791)

Query	1	ACTCTTCATATGTGCTCTCTCTTCACTGTCAA	34
Sbjct	1079	ACTCTTC <u>AAATGTGCTCTCTCCACAATGTCAA</u>	1046
Query	613	...TG <u>GGCGTTATCCCTCTTGAGCTGAGAA</u> -GACAAGGGCTCCCTCTAGGGGGCAAATAG	
Sbjct	425	...TG <u>GGCGTTATCCCTCTTGAGCTGAGAAAGAGAAGGGGA</u> -----AGGGGGTGATCACCG	
Query		GTGAGCTGGGTACACCTGTTAGCGGGGTGTTAACCATTTGAATGCAACACTCCTACGCA	
Sbjct		GAGTCGAAGGG-CGCCTGTTAGCGGGGTGTTAACGACTAATATGGCACTGCGCTTA	
Query		AGACCCTAGCTATGGCTCCA <u>TAGGGTGTGATGAGTGCTTCATCCGGTGCTTCTACTGC</u>	
Sbjct		AGACGTCAGCTATGGCTCC <u>TAGGGTGTGATGAGTGCTTCATCCGGTGCTTCTACTGC</u>	
Query		CTT <u>GCCCCACCTACCCTTGTGATATGGGCCGCGCTGTCGCGTGT-CT-CCTGTATCGGT</u>	
Sbjct		CCA <u>GCCCCACCTACCCTTGTGACATGGCCGTC-TCTCC-CGAGCACGGCCCGTCAAT</u>	
Query		TGTATATCACTCCTGAGCTA	869
Sbjct		TGTATATCACTCCTGAGCTA	176

Figure 6 Pairwise sequence comparisons of selected nucleotide sequences of TAS6/TAS3-like loci from mosses with TAS6/TAS3 of *Physcomitrella patens* precursor RNA (accession JN674513). BLASTN was used at 1 KP blast site. The miR390 target sites are in yellow; putative miR156/miR529 sites are underlined; tasiAP2 is in blue; putative tasiARF-a2 site is in green; tasiARF-a3 is shaded.

Full-size DOI: 10.7717/peerj.4636/fig-6

2050742 *Hedwigia ciliata* (accession YWNF_2050742)

Query 1	ACTCTTCATATGTGCTCTCTCTTCACTGTCAA	34
Sbjct 1070	ACTCTTCAATGTGCTCTCTCCACAAATGTCAA	1037
Query 165	... <u>GTGATCACTCTCTGTCAA</u>	185
Sbjct 885	... <u>GTGATCACTCTCTGTCAA</u>	865
Query 613	...TGGCGTTATCCCTTGTAGCTGAGCTGAGAAGACAAGGGCTCCCTCCTAGG-GGGCGAAAATAG	
Sbjct 431	...TGGCGTTATCCCTTGTAGCTGAGCTGAGAAAAGAAAGTAAGGGTG--AGGAGGGTGGAAAC-G	
Query	GTGAGCTGGGTACACCTTGTAGCGGGGTGTTAACGATTTGAATGCAACACTCCTACGCA	
Sbjct	G---GCCGGCGTC---TTGTAGCGGGGTGTTAACGACTAGCGTGGACACTGCCCTTA	
Query	AGACCCCTAGCTATGGCTCCA <u>TAGGGTGTGATGAGTGCTTCATCCGGTGCTTTCTACTGC</u>	
Sbjct	AGACGTTAGCTACAACATTGTAGGGTGTGATGAGTGCTTACCTGGTGCTCATCCTCTGC	
Query	CTT <u>GCCCACCTACCCTTGTGATA</u> TGGGCCGCGCGTCTGCG-TGTCTCCTGTATCGTT	
Sbjct	CCA <u>GCCCACCTACCCTTGTGACA</u> TGGGCCG-GCCTCTCCGGTGGCCCTTGTCACT	
Query	<u>GTATATCACTCCTGAGCTA</u> 869	
Sbjct	<u>GTATATCACTCCTGAGCTA</u> 183	

2069791 *Diphyscium foliosum* (accession AWOI_2069791)

Query 1	ACTCTTCATATGTGCTCTCTCTTCACTGTCAAAGACCTCGTT	44
Sbjct 302	ACTCTTC <u>CAGATGTGTTCTCTCTCACTGTCA</u> TGACCCCCACTT	345
Query 568	...CGATGTTACGGTTAGCCAATTCTTGTGCACTTAGATTCCACTGGCGTTATCCCTC 627	
Sbjct 853	...CGATGGT--GGATGTAGTCATT-TTCTTGTAA--TAGAGTACCTCA <u>GGCGGTATCCTTC</u> 907	
Query 628	<u>TTGAGCTGAGAA-GA---CAAGGGCTCCCTCTAGGGGGCGAAAATAGGTGA-GCTGGGG</u> 682	
Sbjct 908	<u>CTGAGCTGAGAAAGAGGCCAAGG---CCCT--TAGGG--CAGAAATAGGTGAAGCTGACG</u> 960	
Query 683	TCACCTTGTAG-CGGGTGTTAACGATTTGAATGCAACACTCCTACGC-AAGACCTAG 740	
Sbjct 961	TG---TTGT-AGACTGTGTTAGACACATGAGTAAACACATCGG-GCTAAGACGTACG 1015	
Query 741	CTATGGCTCCATAGGGTGTGATGAGTGCTTCATCCGGTGCTCTCTACTGCCTT <u>GCCCAC</u> 800	
Sbjct 1016	CTATGTCTTCATAGGGTGTGATGAGTGCTTACCCGACGCTCATCTACTGCCA <u>GCCCAC</u> 1075	
Query 801	<u>CTACCCCTGTGATA</u> TGGGCCGCGCGTCTGCGTG-TCTCCTGTATCGGT <u>TGTATATCAC</u> 859	
Sbjct 1076	<u>CTACCCCTGGGACA</u> AGGGCTGTGCAAATTGTGCGGTCC-TATCGGTGTATATCAC 1134	
Query 860	<u>TCCTGAGCTA</u> 869	
Sbjct 1135	<u>TCCTGAGCTA</u> 1144	

Figure 6 (...continued)

Table 3 List of the putative TAS6/TAS3 loci of Bryophyta in transcribed sequences found in 1 KP database.

Plant species	Class/subclass	Order	Length ^a and type	Sequence source
<i>Timmia austriaca</i>	Bryopsida/Timmiidae	Timmiales	TAS6/TAS3 (874 nts)	ZQRI-2061439 ZQRI-2063082
<i>Thuidium delicatulum</i>	Bryopsida/Bryidae	Hypnales	TAS6/TAS3 (837 nts)	EEMJ-2003175
<i>Hypnum subimponens</i>	Bryopsida/Bryidae	Hypnales	TAS6/TAS3 (823 nts)	LNSF-2068452
<i>Pseudotaxiphyllum elegans</i>	Bryopsida/Bryidae	Hypnales	TAS6/TAS3 (1,590 nts)	QKQO-2009669
<i>Anomodon attenuatus</i>	Bryopsida/Bryidae	Hypnales	TAS6/TAS3 (843 nts)	QMWB-2059873
<i>Anomodon rostratus</i>	Bryopsida/Bryidae	Hypnales	TAS6/TAS3 (829 nts)	VBMM-2003482
<i>Schwetschkeopsis fabronia</i>	Bryopsida/Bryidae	Hypnales	TAS6/TAS3 (854 nts)	IGUH-2166854
<i>Leucodon sciuroides</i>	Bryopsida/Bryidae	Hypnales	TAS6/TAS3 (852 nts)	ZACW-2016434
<i>Fontinalis antipyretica</i>	Bryopsida/Bryidae	Hypnales	TAS6/TAS3 (1,410 nts)	DHWX-2007057
<i>Rhytidadelphus loreus</i>	Bryopsida/Bryidae	Hypnales	TAS6/TAS3 (830 nts)	WSPM-2009782
<i>Rhynchostegium serrulatum</i>	Bryopsida/Bryidae	Hypnales	TAS6/TAS3 (853 nts)	JADL-2047695
<i>Climacium dendroides</i>	Bryopsida/Bryidae	Hypnales	TAS6/TAS3 (809 nts)	MIRS-2012325
<i>Calliergon cordifolium</i>	Bryopsida/Bryidae	Hypnales	TAS6 (95 nts)	TAVP-2006322
<i>Neckera douglasii</i>	Bryopsida/Bryidae	Hypnales	TAS6/TAS3 (839 nts)	TMAJ-2023603
<i>Plagiomnium insigne</i>	Bryopsida/Bryidae	Bryales	TAS6/TAS3 (914 nts)	BGXB-2010105
<i>Orthotrichum lyellii</i>	Bryopsida/Bryidae	Orthotrichales	TAS6 (192 nts)	CMEQ-2080784
<i>Hedwigia ciliata</i>	Bryopsida/Bryidae	Hedwigiales	TAS6/TAS3 (877 nts)	YWNF-2050742
<i>Philonotis fontana</i>	Bryopsida/Bryidae	Bartramiales	TAS6/TAS3 (893 nts)	ORKS-2058791
<i>Aulacomnium heterostichum</i>	Bryopsida/Bryidae	Rhizogoniales	TAS6/TAS3 (863 nts)	WNGH-2088134
<i>Scouleria aquatic</i>	Bryopsida/Dicranidae	Scouleriales	TAS6/TAS3 (partial)	BPSG-2088977
<i>Syntrichia princeps</i>	Bryopsida/Dicranidae	Pottiales	TAS6/TAS3 (partial)	GRKU-2074985
<i>Leucobryum glaucum</i>	Bryopsida/Dicranidae	Dicraeales	TAS6/TAS3 (763 nts)	RGKI-2062694
<i>Leucobryum albidum</i>	Bryopsida/Dicranidae	Dicraeales	TAS6/TAS3 (763 nts)	VMXJ-2128109
<i>Dicranum scoparium</i>	Bryopsida/Dicranidae	Dicraeales	TAS6 (105 nts)	NGTD-2092412
<i>Ceratodon purpureus</i>	Bryopsida/Dicranidae	Pseudoditrichales	TAS6/TAS3 (1,121 nts)	FFPD-2005850 SRX2065999
<i>Racomitrium varium</i>	Bryopsida/Dicranidae	Grimmiales	TAS6/TAS3 (724 nts)	RDOO-2117129
<i>Physcomitrium_sp.</i>	Bryopsida/Funariidae	Funariales	TAS6 (partial)	YEPO-2071108
<i>Physcomitrium_sp.</i>	Bryopsida/Funariidae	Funariales	TAS6 (178 nts)	YEPO-2000016
<i>Physcomitrium_sp.</i>	Bryopsida/Funariidae	Funariales	TAS6/TAS3 (821 nts)	YEPO-2016361
<i>Encalypta streptocarpa</i>	Bryopsida/Funariidae	Encalyptales	TAS6/TAS3 (883 nts)	KEFD-2058811
<i>Diphyscium foliosum</i>	Bryopsida/Diphysciidae	Diphyscales	TAS6/TAS3 (832 nts)	AWOI-2069791
<i>Tetraphis pellucida</i>	Tetraphidopsida	Tetraphidales	TAS6 (partial)	HVBQ-2112923
<i>Atrichum angustatum</i>	Polytrichopsida	Polytrichales	TAS6/TAS3 (810 nts)	ZTHV-2082998
<i>Andreaea rupestris</i>	Andreaeopsida	Andreaeales	TAS6/TAS3 (869 nts)	WOGB-2010369
<i>Takakia lepidozoides</i>	Takakiopsida	Takakiales	TAS6/TAS3 (1,040 nts)	SKQD-2076588

Notes.

^aThe length indicates total size of TAS6-TAS3 complex element (from the 5' miR529 target site in TAS6 to 3' miR390 target site in TAS3) or isolated TAS6 (between miR529 and miR156 target sites).

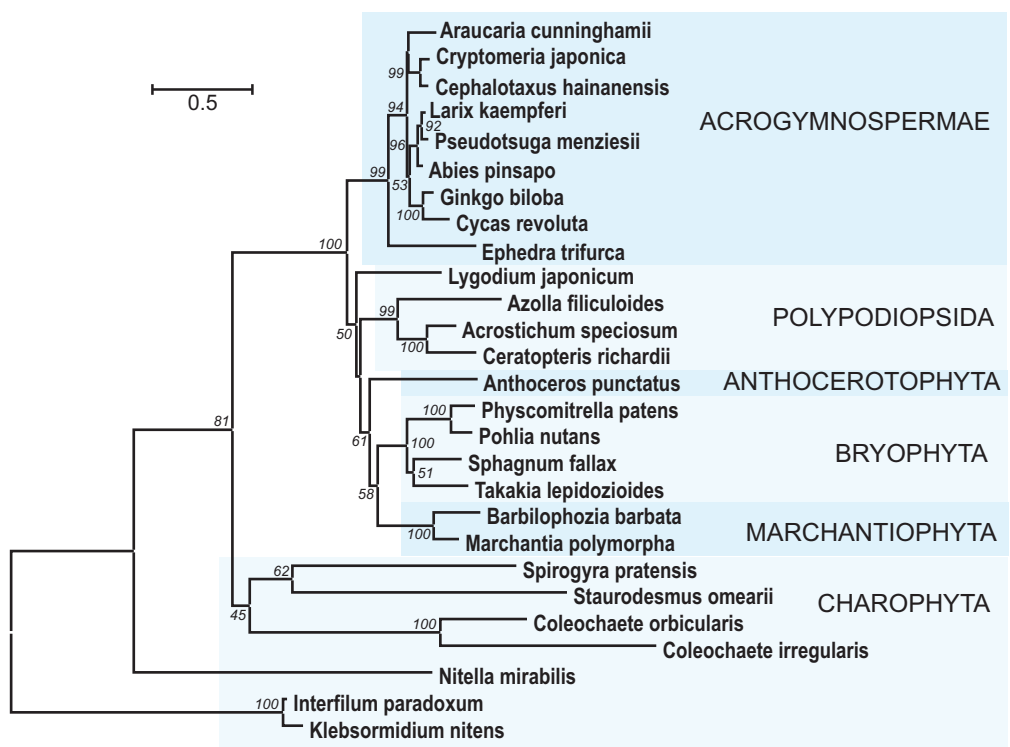


Figure 7 The phylogenetic tree constructed from conserved regions of SGS3 protein sequences from 27 selected streptophytes by the Neighbor-Joining method with 1000 bootstrap replications. There were a total of 419 positions in the final dataset. Evolutionary analyses were conducted in MEGA7 (Kumar, Stecher & Tamura, 2016). Bootstrap support values $\geq 50\%$ are shown. The evolutionary distances were computed using the JTT matrix-based method and are in the units of the number of amino acid substitutions per site. The rate variation among sites was modeled with a gamma distribution (shape parameter = 1). The tree was rooted at two Klebsormidiaceae charophytes. Accession numbers from NCBI or PHYTOZONE data banks see in Fig. S5.

Full-size DOI: 10.7717/peerj.4636/fig-7

XS domain (Bateman, 2002; Zhang & Trudeau, 2008). Importantly, the short N-terminal zf-XS domain is characteristic for functional SGS3 proteins, since the XS domain-containing protein of *Selaginella moellendorffii* lacking TAS-generating machinery (Banks et al., 2011) possesses no zf-XS domain upstream of XS domain and instead contains the C-terminal RING zf region (see NCBI accession XP_002979112). However, it should be noted that the lack of TAS3 pathway and SGS3 is not universal for lycophtyes (Xia, Xu & Meyers, 2017).

In addition to class Bryopsida, SGS3 protein sequences were revealed for members of classes Marchantiopsida, Jungermanniopsida, Anthocerotopsida, Takakiopsida and Sphagnopsida (Fig. 7 and Fig. S5). Most importantly, search for the SGS3 coding sequences in transcriptomes of four charophyte classes (Klebsormidiophyceae) also revealed the SGS3-like proteins in representatives of all these taxa (Fig. 7, Figs. S5, S6). This observation was in agreement with the fact that SGS3-like coding sequence was found in the fully sequenced and annotated genome of *Klebsormidium nitens* (NCBI accession GAQ92898) (Hori et al.,

2014). Moreover, the characteristic motifs of land plant SGS3 proteins (Bateman, 2002) were revealed in the protein sequences from charophyte algae (Figs. S5, S6).

Importantly, in the dendrogram based on comparisons of 27 aligned SGS3 protein sequences, the position of charophytes (Fig. 7) nearly corresponded to the commonly accepted Viridiplantae phylogenetic tree (Shaw, Szövényi & Shaw, 2011; Delwiche & Cooper, 2015; Harrison, 2017), where class Zygnemophyceae (*Spirogyra pratensis*) was a sister group for all land plants. It has become clear that evolving the SGS3-like genes was not directly connected to the appearance of TAS loci in Viridiplantae, since Chlorophyta species, lacking SGS3, encode not only critical enzyme machinery including DCLs, RDRs, and AGOs (You et al., 2017), but also PHAS loci (Zheng et al., 2015). Despite our extensive searches, no SGS3 genes could be identified also in brown and red algae, and this is in agreement with previously published data on green algae (Zheng et al., 2015).

DISCUSSION

Our current analyses revealed previously undiscovered TAS3 loci in bryophytes from classes Takakiopsida, Sphagnopsida and Anthocerotopsida. In *Folioceros fuciformis* (family Anthocerotaceae) we found a TAS3-like sequence which is obviously similar to Bryopsida class III TAS3 species (Fig. 3), whereas Takakiopsida TAS3 locus showed relatedness to class II of TAS3 with typical positioning of tasiAP2 and tasiARF-a2 sequences and no tasiARF-a3 sites (Xia, Xu & Meyers, 2017). Unexpectedly, all predicted Sphagnopsida TAS3 loci showed no conventional internal structural organization of the moss class II and class III TAS3 species. Excepting miR390-targeting regions, the only recognizable conserved site was tasiARF-a2 sequence (Fig. 2).

It was shown that structural organization of Marchantiopsida and Jungermanniopsida TAS3 loci were quite similar, whereas Marchantiophyta TAS3 species were obviously different from those of Bryophyta. These loci were proposed to belong to TAS3 class I with species containing two conserved sequence blocks which presumably represent functional ta-siRNAs (Xia, Xu & Meyers, 2017). One of these blocks was found in the vicinity of the 3'-terminal miR390 binding site and corresponded to Bryopsida tasi-AP2 sequence (Krasnikova et al., 2013), whereas another one (tasiARF-a1), unique among lower land plants, was located closer to the 5'-terminal miR390 binding site in Marchantiopsida and Jungermanniopsida TAS3 (Tsuzuki et al., 2016; Xia, Xu & Meyers, 2017) (Fig. 5, Fig. S3).

Assuming occurrence of tasiARFs as potential products of TAS3 in all main lineages of land plants (Marchantiophyta, Anthocerotophyta and Bryophyta), recent paper proposed that the earliest function of TAS3 could contribute to the production of ta-siRNAs targeting ARF genes, and, since green algae encode no ARF genes, TAS3 likely appeared first in land plants (Xia, Xu & Meyers, 2017). However, extensive comparative sequence analysis showed that charophyte algae representing the sister group to all land plants (colonized terrestrial environments approximately 480 million years ago, see for references Fischer (2018) and Puttick et al. (2018)) could also encode ARF-like proteins including all sequence domains typical for bryophyte and angiosperm ARFs (Mutte et al., 2017). Moreover, our current data showed that TAS3-like loci are encoded by the representatives of all main

taxa among non-vascular plants. These observations suggest that the TAS3 evolution started in a common ancestor of land plants, likely belonging to a still unknown lineage of charophytes. Identification of the canonical motifs of land plant SGS3 in charophyte proteins (see above) indirectly supports this speculation. However, it should be kept in mind that evolving the SGS3-like genes could not be connected solely to the appearance of PHAS loci in Viridiplantae, since green algae and brown algae species were found to encode not only essential silencing machinery enzymes including DCLs, RDRs and AGOs, but also PHAS loci ([Billoud et al., 2014](#); [Zheng et al., 2015](#); [Singh et al., 2015](#); [Dueck et al., 2016](#); [You et al., 2017](#); [Cock et al., 2017](#)). Finally, it can be proposed that the failure to identify charophyte TAS3 loci may be related to (i) the incompleteness of the available sequence data; (ii) evolving by charophytes the one-hit TAS3 genes ([De Felippe et al., 2017](#)); or (iii) the use of miRNA species with sequences other than land plant miR390 for TAS precursor processing.

CONCLUSIONS

The current data on the structural organization of TAS3-like loci in all main classes of land non-vascular plants reveal three types of TAS3 loci, namely, (i) Bryopsida-like TAS3 (classes II and III, [Xia, Xu & Meyers, 2017](#)) found in Bryophyta plants (excepting Sphagnopsida) and Anthocerotopsida, (ii) Marchantiophyta-like TAS3 (class I, [Xia, Xu & Meyers, 2017](#)) and (iii) Sphagnopsida-like TAS3 (this paper). Clearly recognizable common ta-siRNAs is represented in these TAS3 types by tasiARF sequences. Occurrence of primitive SGS3 and ARF genes in charophytes ([Mutte et al., 2017](#) and this paper) supports the idea that TAS3-like genes first appeared in the hypothetical common precursor of land plants ([Xia, Xu & Meyers, 2017](#)) to regulate auxin signaling ([Leyser, 2018](#)).

ACKNOWLEDGEMENTS

We thank researchers who contributed samples used in this study to the 1KP initiative.

ADDITIONAL INFORMATION AND DECLARATIONS

Funding

The work of Sergey Morozov, Tatiana Erokhina and Andrey Solovyev was supported by the Russian Science Foundation (grant 17-14-01032). The work of Irina Milyutina and Alexey Troitsky was supported by the Russian Foundation for Basic Research (grant 18-04-00574-a). The work of Liudmila Ozerova was supported by the State Assignment of MBG RAS on the base of the Unique Scientific Installation “The Fund Greenhouse”. The funders had no role in study design, data collection and analysis, decision to publish, or preparation of the manuscript.

Grant Disclosures

The following grant information was disclosed by the authors:

Russian Science Foundation: 17-14-01032.

Russian Foundation for Basic Research: 18-04-00574-a.

State Assignment of MBG RAS on the base of the Unique Scientific Installation “The Fund Greenhouse”.

Competing Interests

The authors declare there are no competing interests.

Author Contributions

- Sergey Y. Morozov conceived and designed the experiments, analyzed the data, prepared figures and/or tables, authored or reviewed drafts of the paper, approved the final draft.
- Irina A. Milyutina conceived and designed the experiments, performed the experiments, contributed reagents/materials/analysis tools, approved the final draft.
- Tatiana N. Erokhina and Liudmila V. Ozerova performed the experiments, contributed reagents/materials/analysis tools, prepared figures and/or tables, approved the final draft.
- Alexey V. Troitsky and Andrey G. Solovyev conceived and designed the experiments, analyzed the data, authored or reviewed drafts of the paper, approved the final draft.

DNA Deposition

The following information was supplied regarding the deposition of DNA sequences:

New sequences described here are accessible via GenBank accession numbers [MF682529](#) and [MF682530](#).

Supplemental Information

Supplemental information for this article can be found online at <http://dx.doi.org/10.7717/peerj.4636#supplemental-information>.

REFERENCES

- Alaba S, Piszczalka P, Pietrykowska H, Pacak AM, Sierocka I, Nuc PW, Singh K, Plewka P, Sulkowska A, Jarmolowski A, Karlowski WM, Szweykowska-Kulinska Z. 2015. The liverwort *Pellia endiviifolia* shares microtranscriptomic traits that are common to green algae and land plants. *New Phytology* **206**:352–367
[DOI 10.1111/nph.13220](https://doi.org/10.1111/nph.13220).
- Allen E, Howell M. 2010. miRNAs in the biogenesis of trans-acting siRNAs in higher plants. *Seminars in Cell and Developmental Biology* **21**:798–804
[DOI 10.1016/j.semcdb.2010.03.008](https://doi.org/10.1016/j.semcdb.2010.03.008).
- Allen E, Xie Z, Gustafson A, Carrington J. 2005. MicroRNA-directed phasing during trans-acting siRNA biogenesis in plants. *Cell* **121**:207–221
[DOI 10.1016/j.cell.2005.04.004](https://doi.org/10.1016/j.cell.2005.04.004).
- Arif MA, Fattash I, Ma Z, Cho SH, Beike AK, Reski R, Axtell MJ, Frank W. 2012. DICER-LIKE3 activity in Physcomitrella patens DICER-LIKE4 mutants causes severe developmental dysfunction and sterility. *Molecular Plant* **5**:1281–1294
[DOI 10.1093/mp/sss036](https://doi.org/10.1093/mp/sss036).

- Arif MA, Frank W, Khraiwesh B.** 2013. Role of RNA interference (RNAi) in the Moss *Physcomitrella patens*. *International Journal of Molecular Sciences* **14**:1516–1540 DOI [10.3390/ijms14011516](https://doi.org/10.3390/ijms14011516).
- Axtell MJ.** 2013. Classification and comparison of small RNAs from plants. *Annual Review of Plant Biology* **64**:137–159 DOI [10.1146/annurev-arplant-050312-120043](https://doi.org/10.1146/annurev-arplant-050312-120043).
- Axtell MJ, Meyers BC.** 2018. Revisiting criteria for plant miRNA annotation in the era of big data. *The Plant Cell* **30**:272–284 DOI [10.1105/tpc.17.00851](https://doi.org/10.1105/tpc.17.00851).
- Banks JA, Nishiyama T, Hasebe M, Bowman JL, Gribskov M, DePamphilis C, Albert VA, Aono N, Aoyama T, Ambrose BA, Ashton NW, Axtell MJ, Barker E, Barker MS, Bennetzen JL, Bonawitz ND, Chapple C, Cheng C, Correa LG, Dacre M, DeBarry J, Dreyer I, Elias M, Engstrom EM, Estelle M, Feng L, Finet C, Floyd SK, Frommer WB, Fujita T, Gramzow L, Guttensohn M, Harholt J, Hattori M, Heyl A, Hirai T, Hiwatashi Y, Ishikawa M, Iwata M, Karol KG, Koehler B, Kolukisaoglu U, Kubo M, Kurata T, Lalonde S, Li K, Li Y, Litt A, Lyons E, Manning G, Maruyama T, Michael TP, Mikami K, Miyazaki S, Morinaga S, Murata T, Mueller-Roeber B, Nelson DR, Obara M, Oguri Y, Olmstead RG, Onodera N, Petersen BL, Pils B, Prigge M, Rensing SA, Riao-Pachn DM, Roberts AW, Sato Y, Scheller HV, Schulz B, Schulz C, Shakirov EV, Shibagaki N, Shinohara N, Shippen DE, Sørensen I, Sotooka R, Sugimoto N, Sugita M, Sumikawa N, Tanurdzic M, Theissen G, Ulvskov P, Wakazuki S, Weng JK, Willats WW, Wipf D, Wolf PG, Yang L, Zimmer AD, Zhu Q, Mitros T, Hellsten U, Loqu D, Ottillar R, Salamov A, Schmutz J, Shapiro H, Lindquist E, Lucas S, Rokhsar D, Grigoriev IV.** 2011. The selaginella genome identifies genetic changes associated with the evolution of vascular plants. *Science* **332**:960–963 DOI [10.1126/science.1203810](https://doi.org/10.1126/science.1203810).
- Bateman A.** 2002. The SGS3 protein involved in PTGS finds a family. *BMC Bioinformatics* **3**:21 DOI [10.1186/1471-2105-3-21](https://doi.org/10.1186/1471-2105-3-21).
- Billoud B, Nehr Z, Le Bail A, Charrier B.** 2014. Computational prediction and experimental validation of microRNAs in the brown alga *Ectocarpus siliculosus*. *Nucleic Acids Research* **42**:417–429 DOI [10.1093/nar/gkt856](https://doi.org/10.1093/nar/gkt856).
- Bologna N, Voinnet O.** 2014. The diversity, biogenesis, and activities of endogenous silencing small RNAs in *Arabidopsis*. *Annual Review of Plant Biology* **65**:473–503 DOI [10.1146/annurev-arplant-050213-035728](https://doi.org/10.1146/annurev-arplant-050213-035728).
- Borges F, Martienssen RA.** 2015. The expanding world of small RNAs in plants. *Nature Reviews Molecular Cell Biology* **16**:727–741 DOI [10.1038/nrm4085](https://doi.org/10.1038/nrm4085).
- Bowman JL, Kohchi T, Yamato KT, Jenkins J, Shu S, Ishizaki K, Yamaoka S, Nishihama R, Nakamura Y, Berger F, Adam C, Aki SS, Althoff F, Araki T, Arteaga-Vazquez MA, Balasubramanian S, Barry K, Bauer D, Boehm CR, Briginshaw L, Caballero-Perez J, Catarino B, Chen F, Chiyoda S, Chovatia M, Davies KM, Delmans M, Demura T, Dierschke T, Dolan L, Dorantes-Acosta AE, Eklund DM, Florent SN, Flores-Sandoval E, Fujiyama A, Fukuzawa H, Galik B, Grimanelli D, Grimwood J, Grossniklaus U, Hamada T, Haseloff J, Hetherington AJ, Higo A, Hirakawa Y, Hundley HN, Ikeda Y, Inoue K, Inoue SI, Ishida S, Jia Q, Kakita M, Kanazawa T, Kawai Y, Kawashima T, Kennedy M, Kinose K, Kinoshita T, Kohara Y, Koide E,**

Komatsu K, Kopischke S, Kubo M, Kyozuka J, Lagercrantz U, Lin SS, Lindquist E, Lipzen AM, Lu CW, De Luna E, Martienssen RA, Minamino N, Mizutani M, Mizutani M, Mochizuki N, Monte I, Mosher R, Nagasaki H, Nakagami H, Naramoto S, Nishitani K, Ohtani M, Okamoto T, Okumura M, Phillips J, Pollak B, Reinders A, Rvekamp M, Sano R, Sawa S, Schmid MW, Shirakawa M, Solano R, Spunde A, Suetsugu N, Sugano S, Sugiyama A, Sun R, Suzuki Y, Takenaka M, Takezawa D, Tomogane H, Tsuzuki M, Ueda T, Umeda M, Ward JM, Watanabe Y, Yazaki K, Yokoyama R, Yoshitake Y, Yotsui I, Zachgo S, Schmutz J. 2017. Insights into land plant evolution garnered from the *marchantia polymorpha* genome. *Cell* 171:287–304 DOI [10.1016/j.cell.2017.09.030](https://doi.org/10.1016/j.cell.2017.09.030).

Cho SH, Coruh C, Axtell MJ. 2012. miR156 and miR390 regulate tasiRNA accumulation and developmental timing in *Physcomitrella patens*. *The Plant Cell* 24:4837–4849 DOI [10.1105/tpc.112.103176](https://doi.org/10.1105/tpc.112.103176).

Chorostecki U, Moro B, Rojas AML, Debernardi JM, Schapire AL, Notredame C, Palatnik JF. 2017. Evolutionary footprints reveal insights into plant microRNA biogenesis. *The Plant Cell* 29:1248–1261 DOI [10.1105/tpc.17.00272](https://doi.org/10.1105/tpc.17.00272).

Cock JM, Liu F, Duan D, Bourdareau S, Lipinska AP, Coelho SM, Tarver JE. 2017. Rapid evolution of microRNA loci in the brown algae. *Genome Biology and Evolution* 9:740–749 DOI [10.1093/gbe/evx038](https://doi.org/10.1093/gbe/evx038).

Delwiche CF, Cooper ED. 2015. The evolutionary origin of terrestrial life. *Current Biology* 25:R899–R910 DOI [10.1016/j.cub.2015.08.029](https://doi.org/10.1016/j.cub.2015.08.029).

De Felippes FF, Marchais A, Sarazin A, Oberlin S, Voinnet O. 2017. A single miR390 targeting event is sufficient for triggering TAS3-tasiRNA biogenesis in *Arabidopsis*. *Nucleic Acids Research* 45:5539–5554 DOI [10.1093/nar/gkx119](https://doi.org/10.1093/nar/gkx119).

Deng P, Muhammad S, Cao M, Wu L. 2018. Biogenesis and regulatory hierarchy of phased small interfering RNAs in plants. *Plant Biotechnology Journal* DOI [10.1111/pbi.12882](https://doi.org/10.1111/pbi.12882).

Dueck A, Evers M, Henz SR, Unger K, Eichner N, Merkl R, Berezikov E, Engelmann JC, Weigel D, Wenzl S, Meister G. 2016. Gene silencing pathways found in the green alga *Volvox carteri* reveal insights into evolution and origins of small RNA systems in plants. *BMC Genomics* 17:853 DOI [10.1186/s12864-016-3202-4](https://doi.org/10.1186/s12864-016-3202-4).

Fei Q, Xia R, Meyers B. 2013. Phased, secondary, small interfering RNAs in posttranscriptional regulatory networks. *The Plant Cell* 25:2400–2415 DOI [10.1105/tpc.113.114652](https://doi.org/10.1105/tpc.113.114652).

Fischer WW. 2018. Early plants and the rise of mud. *Science* 359:994–995 DOI [10.1126/science.aas9886](https://doi.org/10.1126/science.aas9886).

Harrison CJ. 2017. Development and genetics in the evolution of land plant body plans. *Philosophical Transactions of the Royal Society B: Biological Sciences* 372:20150490 DOI [10.1098/rstb.2015.0490](https://doi.org/10.1098/rstb.2015.0490).

Hori K, Maruyama F, Fujisawa T, Togashi T, Yamamoto N, Seo M, Sato S, Yamada T, Mori H, Tajima N. 2014. Klebsormidium flaccidum genome reveals primary factors for plant terrestrial adaptation. *Nature Communications* 5:3978 DOI [10.1038/ncomms4978](https://doi.org/10.1038/ncomms4978).

- Katoh K, Standley DM.** 2014. MAFFT Multiple sequence alignment software version 7: improvements in performance and usability. *Molecular Biology and Evolution* 30:772–780 DOI [10.1093/molbev/mst010](https://doi.org/10.1093/molbev/mst010).
- Komiya R.** 2017. Biogenesis of diverse plant phasiRNAs involves an miRNA-trigger and Dicer-processing. *Journal of Plant Research* 130:17–23 DOI [10.1007/s10265-016-0878-0](https://doi.org/10.1007/s10265-016-0878-0).
- Krasnikova M, Goryunov D, Troitsky A, Solovyev A, Ozerova L, Morozov S.** 2013. Peculiar evolutionary history of miR390-guided TAS3-like genes in land plants. *Scientific World Journal* 2013:924153 DOI [10.1155/2013/924153](https://doi.org/10.1155/2013/924153).
- Krasnikova M, Milyutina I, Bobrova V, Ozerova L, Troitsky A, Solovyev A, Morozov S.** 2011. Molecular diversity of mir390-guided trans-acting siRNA precursor genes in lower land plants: experimental approach and bioinformatics analysis. *Sequencing* 2011:703683 DOI [10.1155/2011/703683](https://doi.org/10.1155/2011/703683).
- Krasnikova M, Milyutina I, Bobrova V, Troitsky A, Solovyev A, Morozov S.** 2009. Novel miR390-dependent transacting siRNA precursors in plants revealed by a PCR-based experimental approach and database analysis. *Journal of Biomedicine and Biotechnology* 2011:952304 DOI [10.1155/2009/952304](https://doi.org/10.1155/2009/952304).
- Kumar S, Stecher G, Tamura K.** 2016. MEGA7: molecular evolutionary genetics analysis version 7.0 for bigger datasets. *Molecular Biology and Evolution* 33:1870–1874 DOI [10.1093/molbev/msw054](https://doi.org/10.1093/molbev/msw054).
- Lemieux C, Otis C, Turmel M.** 2016. Comparative chloroplast genome analyses of streptophyte green algae uncover major structural alterations in the klebsormid-iophyceae, coleochaetophyceae and zygnematophyceae. *Frontiers in Plant Science* 7:697 DOI [10.3389/fpls.2016.00697](https://doi.org/10.3389/fpls.2016.00697).
- Lewis LA, Mishler BD, Vilgalys R.** 1997. Phylogenetic relationships of the liverworts (Hepaticae), a basal embryophyte lineage, inferred from nucleotide sequence data of the chloroplast gene *rbcL*. *Molecular Phylogenetics and Evolution* 7:377–393 DOI [10.1006/mpev.1996.0395](https://doi.org/10.1006/mpev.1996.0395).
- Leyser O.** 2018. Auxin signaling. *Plant Physiology* 176:465–479 DOI [10.1104/pp.17.00765](https://doi.org/10.1104/pp.17.00765).
- Lin PC, Lu CW, Shen BN, Lee GZ, Bowman JL, Arteaga-Vazquez MA, Liu LY, Hong SF, Lo CF, Su GM, Kohchi T, Ishizaki K, Zachgo S, Althoff F, Takenaka M, Yamato KT, Lin SS.** 2016. Identification of miRNAs and their targets in the liverwort *marchantia polymorpha* by integrating RNA-seq and degradome analyses. *Plant Cell Physiology* 57:339–358 DOI [10.1093/pcp/pcw020](https://doi.org/10.1093/pcp/pcw020).
- Liu H, Yu H, Tang G, Huang T.** 2018. Small but powerful: function of microRNAs in plant development. *Plant Cell Reports* 37:515–528 DOI [10.1007/s00299-017-2246-5](https://doi.org/10.1007/s00299-017-2246-5).
- Morea EG, Da Silva EM, E Silva GF, Valente GT, Barrera Rojas CH, Vincentz M, Nogueira FT.** 2016. Functional and evolutionary analyses of the miR156 and miR529 families in land plants. *BMC Plant Biology* 16:40 DOI [10.1186/s12870-016-0716-5](https://doi.org/10.1186/s12870-016-0716-5).
- Mutte S, Kato H, Rothfels C, Melkonian M, Wong GK-S, Weijers D.** 2017. Origin and evolution of the nuclear auxin response system. *bioRxiv* 220731 DOI [10.1101/220731](https://doi.org/10.1101/220731).

- Ozerova L, Krasnikova M, Troitsky A, Solovyev A, Morozov S.** 2013. TAS3 genes for small ta-siARF RNAs in plants belonging to subtribe Senecioninae: occurrence of prematurely terminated RNA precursors. *Molekularnaia Genetika, Mikrobiologija I Virusologija* **28**:79–84.
- Plavskin Y, Nagashima A, Perroud PF, Hasebe M, Quatrano RS, Atwal GS, Timmermans MC.** 2016. Ancient trans-acting siRNAs confer robustness and sensitivity onto the auxin response. *Developmental Cell* **36**:276–289 DOI [10.1016/j.devcel.2016.01.010](https://doi.org/10.1016/j.devcel.2016.01.010).
- Puttick MN, Morris JL, Williams TA, Cox CJ, Edwards D, Kenrick P, Pressel S, Wellman CH, Schneider H, Pisani D, Donoghue PCJ.** 2018. The interrelationships of land plants and the nature of the ancestral embryophyte. *Current Biology* **28**:733–745 DOI [10.1016/j.cub.2018.01.063](https://doi.org/10.1016/j.cub.2018.01.063).
- Qiu YL.** 2008. Phylogeny and evolution of charophytic algae and land plants. *Journal of Systematics and Evolution* **46**:287–306 DOI [10.3724/SP.J.1002.2008.08035](https://doi.org/10.3724/SP.J.1002.2008.08035).
- Rogers K, Chen X.** 2013. Biogenesis, turnover, and mode of action of plant microRNAs. *The Plant Cell* **25**:2383–2399 DOI [10.1105/tpc.113.113159](https://doi.org/10.1105/tpc.113.113159).
- Rosato M, Kovářík A, Garilletti R, Rosselló JA.** 2016. Conserved organisation of 45S rDNA sites and rDNA gene copy number among major clades of early land plants. *PLOS ONE* **11**:e0162544 DOI [10.1371/journal.pone.0162544](https://doi.org/10.1371/journal.pone.0162544).
- Ruhfel BR, Gitzendanner MA, Soltis PS, Soltis DE, Burleigh JG.** 2014. From algae to angiosperms—inferring the phylogeny of green plants (Viridiplantae) from 360 plastid genomes. *BMC Evolutionary Biology* **14**:23 DOI [10.1186/1471-2148-14-23](https://doi.org/10.1186/1471-2148-14-23).
- Samigullin TK, Yacentyuk SP, Degtyaryeva GV, Valieho-Roman KM, Bobrova VK, Capesius I, Martin WF, Troitsky AV, Filin VR, Antonov AS.** 2002. Paraphyly of bryophytes and close relationship of hornworts and vascular plants inferred from chloroplast rDNA spacers sequence analysis. *Arctoa* **11**:31–43 DOI [10.15298/arctoa.11.05](https://doi.org/10.15298/arctoa.11.05).
- Santin F, Bhogale S, Fantino E, Grandellis C, Banerjee AK, Ulloa RM.** 2017. Solanum tuberosum StCDPK1 is regulated by miR390 at the posttranscriptional level and phosphorylates the auxin efflux carrier StPIN4 *in vitro*, a potential downstream target in potato development. *Physiologia Plantarum* **159**:244–261 DOI [10.1111/ppl.12517](https://doi.org/10.1111/ppl.12517).
- Shaw AJ, Cox CJ, Buck WR, Devos N, Buchanan AM, Cave L, Seppelt R, Shaw B, Larraín J, Andrus R, Greilhuber J, Temsch EM.** 2010. Newly resolved relationships in an early land plant lineage: Bryophyta class Sphagnopsida (peat mosses). *American Journal of Botany* **97**:1511–1531 DOI [10.3732/ajb.1000055](https://doi.org/10.3732/ajb.1000055).
- Shaw AJ, Szövényi P, Shaw B.** 2011. Bryophyte diversity and evolution: windows into the early evolution of land plants. *American Journal of Botany* **98**:352–369 DOI [10.3732/ajb.1000316](https://doi.org/10.3732/ajb.1000316).
- Shaw AJ, Devos N, Liu Y, Cox CJ, Goffinet B, Flatberg KI, Shaw B.** 2016. Organellar phylogenomics of an emerging model system: Sphagnum (peatmoss). *Annals of Botany* **118**:185–196 DOI [10.1093/aob/mcw086](https://doi.org/10.1093/aob/mcw086).

- Singh RK, Gase K, Baldwin IT, Pandey SP.** 2015. Molecular evolution and diversification of the Argonaute family of proteins in plants. *BMC Plant Biology* **15**:23 DOI [10.1186/s12870-014-0364-6](https://doi.org/10.1186/s12870-014-0364-6).
- Tsuzuki M, Nishihama R, Ishizaki K, Kurihara Y, Matsui M, Bowman JL, Kohchi T, Hamada T, Watanabe Y.** 2016. Profiling and characterization of small rnas in the liverwort, marchantia polymorpha, belonging to the first diverged land plants. *Plant Cell Physiology* **57**:359–372 DOI [10.1093/pcp/pcv182](https://doi.org/10.1093/pcp/pcv182).
- Wickett NJ, Mirarab S, Nguyen N, Warnow T, Carpenter E, Matasci N, Ayyampalayam S, Barker MS.** 2014. Phylogenomic analysis of the origin and early diversification of land plants. *Proceedings of the National Academy of Sciences of the United States of America* **111**:E4859–E4868 DOI [10.1073/pnas.1323926111](https://doi.org/10.1073/pnas.1323926111).
- Xia R, Meyers BC, Liu Z, Beers EP, Ye S, Liu Z.** 2013. MicroRNA superfamilies descended from miR390 and their roles in secondary small interfering RNA Biogenesis in Eudicots. *The Plant Cell* **25**:1555–1572 DOI [10.1105/tpc.113.110957](https://doi.org/10.1105/tpc.113.110957).
- Xia R, Xu J, Meyers BC.** 2017. The emergence, evolution, and diversification of the miR390 TAS3 ARF pathway in land plants. *The Plant Cell* **29**:1232–1247 DOI [10.1105/tpc.17.00185](https://doi.org/10.1105/tpc.17.00185).
- Yoshikawa M.** 2013. Biogenesis of trans-acting siRNAs, endogenous secondary siRNAs in plants. *Genes & Genetic Systems* **88**:77–84 DOI [10.1266/ggs.88.77](https://doi.org/10.1266/ggs.88.77).
- You C, Cui J, Wang H, Qi X, Kuo L-Y, Ma H, Gao L, Mo B, Chen X.** 2017. Conservation and divergence of smallRNA pathways and microRNAs in plants. *Genome Biology* **18**:158 DOI [10.1186/s13059-017-1291-2](https://doi.org/10.1186/s13059-017-1291-2).
- Zhai J, Jeong D, De Paoli E, Park S, Rosen B, Li Y, González A, Yan Z, Kitto S, Grusak M, Jackson S, Stacey G, Cook D, Green P, Sherrier D, Meyers M.** 2011. MicroRNAs as master regulators of the plant NB-LRR defense gene family via the production of phased, trans-acting siRNAs. *Genes & Development* **25**:2540–2553 DOI [10.1101/gad.177527.111](https://doi.org/10.1101/gad.177527.111).
- Zhang D, Trudeau VL.** 2008. The XS domain of a plant specific SGS3 protein adopts a unique RNA recognition motif (RRM) fold. *Cell Cycle* **7**:2268–2270 DOI [10.4161/cc.7.14.6306](https://doi.org/10.4161/cc.7.14.6306).
- Zheng Y, Wang Y, Wu J, Ding B, Fei Z.** 2015. A dynamic evolutionary and functional landscape of plant phased small interfering RNAs. *BMC Biology* **13**:32 DOI [10.1186/s12915-015-0142-4](https://doi.org/10.1186/s12915-015-0142-4).